Intensity of the geomagnetic field in western Europe over the past 2000 years: New data from ancient French pottery

Agnès Genevey, Yves Gallet

Intensity of the geomagnetic field in western Europe over the past 2000 years: New data from ancient French pottery

Agnès Genevey and Yves Gallet

Laboratoire de Paléomagnétisme, Institut de Physique du Globe de Paris, Paris, France

Received 22 June 2001; revised 15 May 2002; accepted 15 May 2002; published 9 November 2002.

[1] We studied 14 groups of French pottery fragments dated between the 4th and 16th centuries. The potsherds were analyzed using the *Thellier and Thellier* [1959] method, revised by *Coe* [1967]. Intensity values were corrected for thermoremanent magnetization (TRM) anisotropy and cooling rate dependence of TRM acquisition. We first analyzed modern ceramics produced following ancient techniques and fired in a wood-burning kiln inside of which field intensity was measured. The recovered mean intensity is within ~3% of the expected value, which proves the reliability of our experimental procedure. Thermal experiments carried out at rapid and slow cooling rates clearly indicate that the cooling rate correction is critical in archeointensity studies. Our data indicate that large variations in intensity occurred in France over the last 2000 years. Two relative maxima in intensity are observed, one between the 8th and 10th centuries and the second between the 14th and 15th centuries. Similarities are observed between the archeointensity data from France and Ukraine, yielding some evidence for eastward drift of geomagnetic sources between western and eastern Europe from A.D. 800 to A.D. 1700. We also show that the dipole moment evolution proposed by *McElhinny and Senanayake* [1982] and *Yang et al.* [2000] for the last two millennia is likely biased toward higher values, mainly because of the absence of correction for the cooling rate dependence of TRM acquisition in most published archeointensity studies. We finally underline a possible relationship, valid at least in western Europe, between changes in direction and intensity of the geomagnetic field. *INDEX TERMS:* 1522 Geomagnetism and Paleomagnetism: Paleomagnetic secular variation; 1503 Geomagnetism and Paleomagnetism: Archeomagnetism; 1521 Geomagnetism and Paleomagnetism: Paleointensity; 9335 Information Related to Geographic Region: Europe; *KEYWORDS:* archeomagnetism, archeointensity, secular variation, western Europe, cooling rate dependence

Citation: Genevey, A., and Y. Gallet, Intensity of the geomagnetic field in western Europe over the past 2000 years: New data from ancient French pottery, *J. Geophys. Res.*, *107*(B11), 2285, doi:10.1029/2001JB000701, 2002.

1. Introduction

[2] Determining the behavior of the time-varying nondipole part of the geomagnetic field requires the acquisition of well dated and widely distributed magnetic measurements at the Earth's surface. This was possible for the past 300 years based on direct geomagnetic measurements made in a few magnetic observatories or by mariners [e.g., *Barraclough*, 1974; *Bloxham and Jackson*, 1992; *Alexandrescu et al.*, 1997]. Prior to historical periods, the secular variation in the geomagnetic field can be scrutinized from the analysis of the remanent magnetization of man-made materials and rocks [*Daly and Le Goff*, 1996]. Using such a data set, *Hongre et al.* [1998] recently computed spherical harmonic models of the geomagnetic field between 0 and A.D. 1700 based on 14 unevenly distributed archeomagnetic and paleomagnetic (volcanic and sedimentary) records [see also *Constable et al.*, 2000]. These models, which incorporate Gauss coefficients up to degree 2 and order 2 plus those of degree 3 and order 3, confirm the significant decrease of the dipole field in the last two thousand years. They also show that the correlation times associated with the degree 2 and 3 coefficients are likely to be less than 200 years, as previously suggested by *Hulot and Le Mouël* [1994] from historical data, further indicating that the nondipole field would be uncorrelated with its past behavior after a period of ~450 years [see also *Carlut et al.*, 1999].

[3] However, possibilities for long-lasting, drifting or standing, nondipole features at timescales of several centuries up to a million years are still strongly debated [e.g., *Courtillot and Le Mouël*, 1988; *Merrill et al.*, 1996; *Carlut and Courtillot*, 1998; *Constable et al.*, 2000]. Reasons for these uncertainties mainly arise from the small number of areas where measurements of the ancient field are presently available. Moreover, these measurements need to meet severe quality criteria, principally a high precision in the determination of the magnetic vector and in the timing of the magnetization acquisition. Among the archeomagnetic data used by *Hongre et al.* [1998], those obtained for France by

0148-0227/02/2001JB000701$09.00

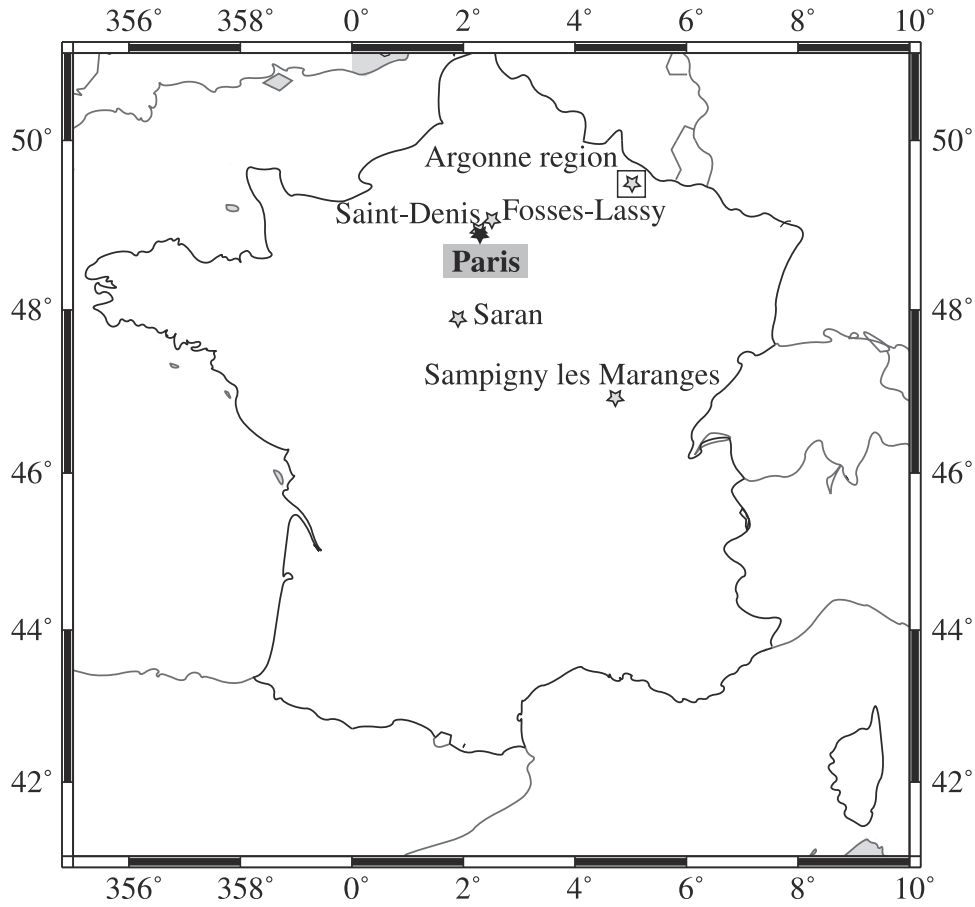

Figure 1. Location of the different sites in France where the pottery fragments were collected.

Thellier [1981] and *Bucur* [1994] yield a detailed record of the directional changes of the geomagnetic field during the last 21 centuries. However, a complete description of the geomagnetic field vector in western Europe is not yet achieved since variations of magnetic field intensity are only poorly known. We recall that direct measurements of geomagnetic field intensity are relatively recent (in historical sense), the first being performed by Carl Friedrich Gauss in 1832, some three centuries after the first measurements of geomagnetic directions in France or in Great Britain [e.g., *Malin and Bullard*, 1981; *Alexandrescu et al.*, 1997].

[4] *Chauvin et al.* [2000] recently compiled the archeointensity results obtained from western Europe for the 0 to A.D. 2000 period. It is remarkable to note that no data are presently available between the end of the Roman empire (5th century) and approximately A.D. 1100. Moreover, the reliability of some existing data obtained for the Middle Ages seems questionable, in particular, between the 12th and 15th centuries, because they are often based on the investigation of very few (one or two) samples per dated site [e.g., *Games and Davey*, 1985]. We have therefore investigated the archeointensity of 14 groups of pottery shards, archeologically dated between the 4th and 16th centuries A.D.. Our study allows the determination of the general evolution of the geomagnetic field intensity in France during the last 2000 years. It is undertaken in the frame of a long-term project which intends to better constrain the dynamics of the fluid inner core from a more detailed description of the geomagnetic field during the last few millennia. As another important application, variations of geomagnetic field intensity could also be helpful for dating archeological structures, with or without the help of the directional changes which are already used in France for this purpose.

2. Selection of Pottery Shards

[5] The selection of the studied groups of pottery shards, each taken from different ceramics, was guided by two main parameters: a clear argument to assume that pottery shards from each group all have the same age, and a good precision on this dating. It is worth noting that when dispersed potsherds are found in occupation context, in particular in domestic dumping grounds, their dating may be uncertain because the fragments (particularly when only a small part of one pottery is found) may have been stratigraphically displaced, for instance because of ancient excavation works. For this reason, we principally selected pottery groups which were found in a production context (Fosses, Saint Denis, and Saran; Figure 1), in direct connection with kilns where these ceramics were baked. For some reasons, such as cracks induced by the firing-cooling process, the failed ceramics were thrown out in the very close vicinity of the kiln. In this case, dating constraints are obtained both from pottery typology based on a large collection of fragments and from the general archeological situation including the

Table 1. Location and Ages of the Different Studied Pottery Groups[a]

Location	Name of Pottery Group	Age, A.D.	Archeological Context of Findings[b]	Dating Criteria					
				Evolution of Ceramic Typology	Stratigraphic Constraints	Coins	Small Objects[c]	Decoration Made With a Toothed-Wheel	Archeo-magnetic Dating
Argonne region									
49.5°N, 5.0°E	A39	[325–350]	O					X	
	A41	[400–425]	O					X	
	A29	[440–480]	O					X	
Saran									
47.9°N, 1.9°E	A36	[700–750]	P	X					
	A38	[800–850]	P	X				X	
Lassy			P						
49.1°N, 2.5°E	A20	[920–1000]	P	X					X
St Denis			P						
48.9°N, 2.4°E	A32	[1300–1350]	P	X			X		
Fosses			P						
49.1°N, 2.5°E	A02	[1100–1150]	P	X	X				
	A07	[1200–1250]	P	X					
	A08	[1250–1300]	P	X	X	X			
	A11	[1300–1350]	P	X		X	X		
	A12	[1350–1400]	P	X	X				
	A16	[1500–1550]	P	X		X			
	A18	[1550–1600]	P	X					
Sampigny les Maranges									
46.9°N, 4.6°E	P number								

[a] Archeological dating criteria available for these groups are also indicated.
[b] O is for occupation layers and P is for production context.
[c] Jewels, glassware, clothing clip, etc.

kiln which independently may provide dating constraints from small objects lost by the craftsmen during their work (coins, clips of clothes, etc.) and from archeomagnetic results. Another advantage of these pottery shards for archeointensity analyses relies on the fact that because the ceramics were never used for cooking, they often present only one magnetic component which simplifies the interpretation of the magnetic data.

[6] Seven groups of pottery shards were found in Fosses, a village located in the Ysieux valley ~30 km to the north of Paris (Figure 1). Another one comes from a close by village in the same valley (Lassy, Table 1). Fosses was an active pottery production center during about 1000 years up to the middle of the 17th century, with a climax during the 12th and the 13th centuries [*Guadagnin*, 2000]. Note that the Fosses ceramics are commonly found in the Ile de France region, for instance, in Paris or in Saint Denis, during archeological excavations. The pottery production ended in Fosses likely when the main clay deposits were exhausted, but it remained in the Ysieux valley, although on a more limited scale, up to the beginning of the 19th century (e.g., in the village of Bellefontaine). About 18 production units, consisting of kilns associated with massive quantities (several tons) of pottery shards, were located and/or excavated in Fosses and in the surrounding countryside during the last 10 years. A detailed description of the findings is given by *Guadagnin* [2000], and Table 1 summarizes the age constraints available for the different studied potsherd groups. We also present archeointensity data obtained from two other archeological sites where kilns and associated ceramics were found: Saran close to the city of Orléans, which was a small pottery production center during the High Middle Ages, and Saint Denis (Figure 1) (S. Jesset and N. Meyer-Rodrigues, personal communications, 2001).

[7] In our study, we have also considered another dating criterion based on the pottery decoration for retaining and analyzing potsherd groups. This criterion, which concerns the four oldest groups of our data set, appears particularly satisfactory because it provides a precise age control for pottery shards found in occupation context and from different archeological sites. We selected three groups of terra sigillata (Samian wares) fragments of the late Roman period coming from the Argonne region (northeastern France, Figure 1). Terra sigillata was a fine pottery of daily usage but rarely used for heating, which ensures in most cases that only one magnetic component will be isolated. Each group is constituted by fragments exhibiting a decoration made with a toothed-wheel, the different decorations being identified and indexed by archeologists. We took advantage of the intensive studies made on the toothed-wheel decoration of the Argonne terra sigillata showing their rapid evolution in time during the 4th and 5th centuries and allowing their dating [e.g., *Van Ossel*, 1996]. This ensures a great temporal homogeneity for each group, which undoubtedly counterbalances the fact that the pottery shards were found in occupation context. In this matter, the most favorable case was met for the A38 group found in Saran. As for the Argonne ceramics, these potsherds taken from different rejected ceramics show the same toothed-wheel decoration. In addition, we know that this decoration was made with the same tool because it had a default which is observed on all fragments. This group thus combines the advantages linked to our different archeological selection criteria. However, if temporal homogeneity is excellent (likely better than 1 year because the toothed wheel was in wood and had to be changed often), the dating of the

whole group is far from being as precise as is currently the case for High Middle Ages archeological sites.

3. Experimental Procedure

[8] Between five and eight samples were analyzed per pottery group. The potsherds were cut into small cubic samples 1 cm × 1 cm × h, with $h < 1$ cm depending on the thickness of the pottery. An arbitrary orientation was given to samples in such a way that their z axis is perpendicular to the shear plane of the pottery clay. Three samples were prepared from each fragment, two for archeointensity determination and one for cooling rate experiments.

3.1. Thermal Treatment and Magnetic Measurements

[9] Archeointensity experiments were carried out in air using the *Thellier and Thellier* [1959] method as revised by *Coe* [1967]. For each double heating step, the samples were first partially remagnetized (pTRM) in a known laboratory field along a direction in the shear plane of the pottery, and next demagnetized in a zero field [*Aitken et al.*, 1988]. During our experiments, we used successively two different ovens. About one fifth of the collection was treated using a first oven, in which the samples were heated in zero field during about 1 hour and then cooled down in a separate zone, with or without an applied field. In order to improve data acquisition, we also employed a new oven of smaller size, better adapted to our archeointensity experiments, in which the samples were heated during 30 min and cooled down at the same place also during 30 min. The cooling of this oven is controlled by a temperature regulator allowing one to impose a specific cooling rate.

[10] Magnetization measurements were carried out in the shielded room of the paleomagnetic laboratory of IPGP with a 2G (horizontal) cryogenic magnetometer. Twelve to 16 double-heating steps were performed from 100°C to 500–550°C depending on natural remanent magnetization (NRM) demagnetization, the temperature interval being 50°C from 100°C to 250°C and 25°C afterward. The pTRM checks were made every two temperature steps in order to detect any alteration in the magnetic mineralogy of the samples. In addition to these experiments, TRM anisotropy and TRM cooling rate dependence were taken into account to correct the raw archeointensity results.

3.2. TRM Anisotropy

[11] The TRM anisotropy observed in pottery shows an easy plane of magnetization which is often within the shear plane of the clay [e.g., *Rogers et al.*, 1979; *Aitken et al.*, 1981]. This anisotropy is therefore interpreted as reflecting preferential alignment of magnetic grains induced by stretching of clay when the ceramics were molded into shape on a wheel. To evaluate the TRM anisotropy effect, we determined for each sample and at two different temperatures, generally when ~30 to 50% and ~60 to 90% of NRM were demagnetized, a TRM anisotropy tensor from which we calculated the correction factor f as defined by *Veitch et al.* [1984]. This TRM tensor was obtained from the acquisition of six TRM by applying a field successively in six different directions relative to the samples (X, -X, Y, -Y, Z, -Z). We further note that the magnetization of our samples is of a few amperes per meter (most often on the order of 1–2 A/m) which allows us to neglect the shape anisotropy [*Lanos*, 1987].

3.3. Cooling Rate Dependence

[12] The cooling rate dependence of TRM acquisition is based on the *Néel* [1955] theory for an assemblage of identical single-domain (SD) grains [see also *Dodson and McClelland-Brown*, 1980; *Halgedahl et al.*, 1980]. This effect, which consists in a progressive increase of TRM intensity as the cooling rate becomes slower, was later experimentally confirmed by several authors for pseudosingle-domain (PSD) grains in baked clays and volcanic rocks [e.g., *Biquand*, 1994; *Chauvin et al.*, 2000]. Samples were obviously cooled down much more rapidly in our archeointensity experiments (in less than 30 min from 500°C to 25°C) than during the original cooling of the studied ceramics. In order to quantify the cooling rate effect, we carried out TRM acquisition experiments both at rapid (cooling rate used in routine in double-heating procedure: 450°C in ~0.5 hour) and slow cooling rates (450°C in ~1.5 day). We used the procedure described by *Garcia* [1996] and *Chauvin et al.* [2000]. It involves, at the same temperature, three series of heatings and coolings in a specific field at rapid, slow and again rapid rates, the last cooling allowing the detection of any significant change in magnetic mineralogy during the treatment. These three heating steps were performed at intermediate temperatures, generally 450°C, for which at least 50% of NRM were removed. We note $\mathbf{TRM_{R1}}$, $\mathbf{TRM_{R2}}$, the TRM acquired after the first and the final rapid cooling, and $\mathbf{TRM_S}$ the TRM acquired after the slow cooling. The correction factor which we applied to the intensity is

$$F_{\text{cooling rate}} = [(\|\mathbf{TRM_{R1}}\| + \|\mathbf{TRM_{R2}}\|)/2]/\|\mathbf{TRM_S}\| = \|\mathbf{TRM_R}\|/\|\mathbf{TRM_S}\| . \quad (1)$$

Moreover, the percentage of evolution during this procedure is estimated by

$$\%\text{evol}_{\text{cooling rate exp.}} = \text{abs}(\|\mathbf{TRM_{R1}}\| - \|\mathbf{TRM_{R2}}\|)/\|\mathbf{TRM_{R1}}\| . \quad (2)$$

The slow cooling rate was chosen to reproduce as faithfully as possible the initial cooling conditions of the ceramics. We used two different slow cooling rates. The first one (33 hours to cool from 450°C to room temperature) corresponds to the cooling rate which likely prevailed in large kilns dated from the Roman Empire and the Middle Ages (as deduced from archeological experiments and from the cooling of our modern ceramics, see section 3.4). In contrast, the ceramics from the site of Saran were baked in kilns with smaller size, and experimental firings in the same kilns indicated that the cooling of the ceramics was accomplished after about half a day (S. Jesset, personal communication, 2001). For these latter samples, we thus considered a slow cooling time of 10 hours to decrease the temperature from 450°C to room temperature.

3.4. Selection Criteria for Archeointensity Determinations

[13] The raw intensity values of the ancient field are obtained from the slopes, determined by least squares

analysis, of linear segments in "NRM lost" versus "TRM gained" ("Arai" [*Nagata et al.*, 1963]) diagrams [*Coe et al.*, 1978]. The segments are defined in the temperature range for which a magnetic component is clearly isolated in the corresponding orthogonal vector diagrams. In addition to the quality of the slopes in Arai diagrams and to successful pTRM checks (we fixed a limit of 10% on evolution), we considered other criteria to better ascertain the reliability of our archeointensity results. First the slope determined in the Arai diagrams must involve more than 40% of the NRM. In all cases, it amounts to considering linear segments defined by at least five temperature steps. Another criterion relates to the coherency of the intensity results obtained from two samples collected from each pottery fragment. A mean archeointensity value is computed for one fragment only if the difference between the two individual values is less than 5%. The difference in TRM acquisition between the two rapid coolings performed in the cooling rate dependence experiments must also not exceed ~5% otherwise the pottery shard is rejected. Finally, each independently dated site must be defined by at least three archeointensity results (i.e., three pottery shards, thus six samples) and the standard deviation of the mean must be less than 5 μT.

4. A Preliminary Test

[14] Ceramics from Fosses were all made with the clay of Ypresian (Eocene) age which widely outcrops in the close vicinity of the village and along the Ysieux valley [e.g., *Guadagnin*, 2000]. This gives us the opportunity to test the ability of our experimental procedure to provide reliable archeointensity results. We asked a pottery craftsman (François Fresnais) working in Savigny les Maranges (Burgundy region, central France) to mold, on a wheel, with the Fosses clay, new ceramics into the most common shapes of the ceramics made in Fosses during the 12th and 13th centuries. These ceramics were baked in a wood-burning kiln during about one day, and then cooled down in about two days. We measured with a fluxgate magnetometer the magnetic field inside the kiln, while it was cold, first empty (44.7 ± 2.6 μT) and then full of ceramics (43.6 ± 2.8 μT).

[15] Isothermal remanent magnetization (IRM) acquisitions indicate that the magnetization of our modern ceramics is still not saturated at fields of 1.2 T, suggesting the presence of a small fraction of hematite together with a mineral of lower coercivity, likely magnetite. A mixture of magnetic minerals with different coercivities is confirmed by hysteresis loops showing a clear wasp-waisted shape (Figure 2a) [e.g., *Dunlop and Özdemir*, 1997]. Five ceramics were sampled for archeointensity analyses. Results on TRM anisotropy and cooling rate dependency will be discussed in section 5 together with ancient samples. All samples show linear segments in Arai diagrams within almost the entire temperature range up to 500°C with positive pTRM checks (Figure 2b). When corrected for the anisotropy effect, the intensity values obtained from the twin samples pass the consistency test and the five potsherds are therefore considered for the general mean computation (Table 2). This mean (42.2 μT) is well defined, with a small standard deviation of 1.1 μT: it agrees well with the magnetic field intensity measured in the kiln full of ceramics. Our result is only ~3% less than the expected value, which demonstrates the reliability of our experimental procedure.

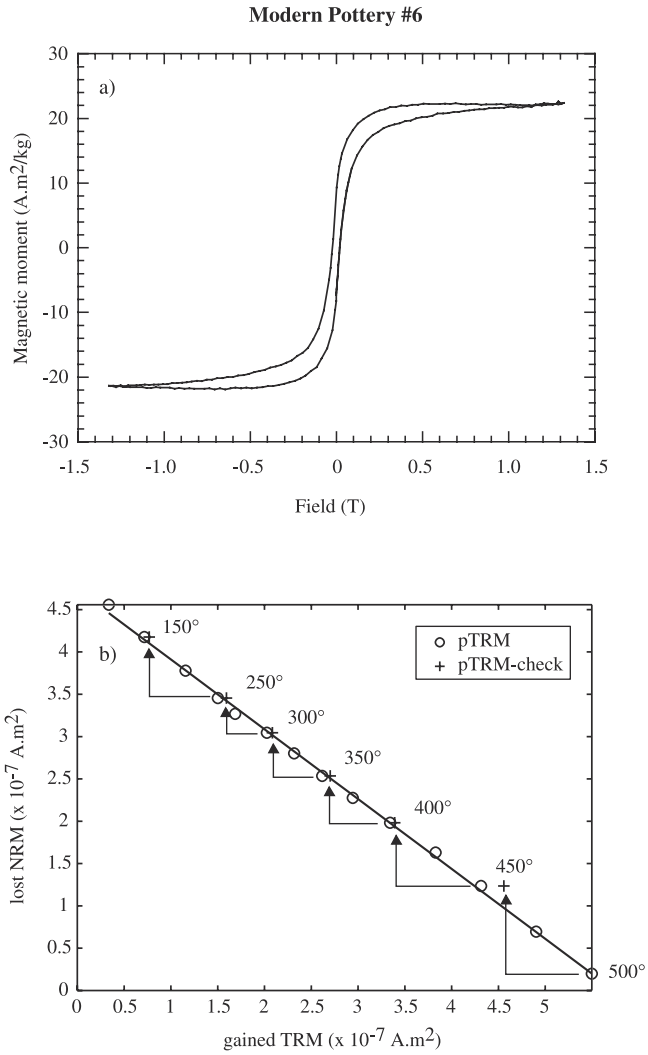

Figure 2. Magnetic analyses carried out on one fragment of modern ceramic. (a) Hysteresis loop showing a wasp-waisted behavior. (b) Typical example of NRM-lost versus TRM-gained diagram (open circles). The crosses indicate the pTRM checks performed every two thermal steps. The slope was determined from the linear segment marked on the Figure.

5. Archeointensity Results

5.1. Magnetic Mineralogy

[16] We carried out hysteresis and IRM measurements on two samples from each potsherd group. Two main behaviors are distinguished from the hysteresis loops on the basis of the occurrence (or not) of a well-developed wasp-waisted shape (Figures 3a and 3c, respectively). This distinction determines whether saturation is reached or not in fields up to 1.2 T (Figures 3b and 3d, respectively). Wasp-waisted shapes are only observed when saturation is not reached, likely indicating the coexistence of magnetite and hematite, as in the case for modern ceramics. In contrast, those

Table 2. Archeointensity Results Obtained From Modern Pottery[a]

Pottery	Samples	n	T_{min}-T_{max}	f	g	q	H Lab	H Noncorrected	σ_H	H Anisotropy Corrected	H Mean Value per Potsherd Corrected for the Cooling Rate Effect	$H_{mean} \pm \sigma_H$
P6	X386	14	100–500	0.92	0.92	80.98	50	41.3	0.4	43.6	40.9 ± 0.4	
	X387	14	100–500	0.90	0.91	64.79	50	39.7	0.5	42.7		
P8	X369	14	100–500	0.91	0.87	75.49	50	44.0	0.5	46.4	42.0 ± 0.2	
	X370	14	100–500	0.91	0.87	67.97	50	44.8	0.5	46.8		
P15	X367	13	100–475	0.96	0.91	51.02	50	42.8	0.7	45.4	42.4 ± 0.2	42.2 ± 1.1
	X368	13	100–475	0.95	0.91	45.80	50	45.8	0.9	45.8		
P19	X371	13	100–475	0.96	0.90	48.05	50	41.5	0.7	44.8	41.7 ± 0.1	
	X372	13	100–475	0.95	0.91	44.64	50	41.1	0.8	44.8		
P21	X373	13	100–475	0.93	0.91	36.94	50	46.9	1.1	47.1	43.9 ± 0.1	
	X374	13	100–475	0.93	0.91	37.96	50	44.9	1.0	47.1		

[a] Here n is the number of heating steps used to determine intensity; T_{min}-T_{max} is the corresponding temperature interval (in °C); f is the fraction factor; g is the gap factor; q is the quality factor; H_{lab} is the intensity of the laboratory field in μT; H noncorrected is the archeointensity before TRM anisotropy and cooling rate corrections in μT; σ_H is the standard error in μT; H anisotropy corrected is the archeointensity after TRM anisotropy correction in μT; H_{mean} value per potsherd corrected for the cooling rate effect in μT, $H_{mean} \pm \sigma_H$ is mean intensity and standard deviation in μT.

samples for which the magnetization is saturated at fields <0.5 T show nonconstricted hysteresis shapes and the measured hysteresis parameters indicate that their magnetization is carried by PSD grains of magnetite [*Day et al.*, 1977]. This magnetic mineralogy appears very similar to the one previously described by several authors for pottery and brick fragments [e.g., *Yang et al.*, 1993; *Evans and Jiang*, 1996; *Chauvin et al.*, 2000].

[17] We also performed bulk susceptibility versus temperature measurements up to 700°C for several samples using CS2 magnetic susceptibility meter, in order to determine the Curie temperature of the magnetic minerals present in our samples. The presence of a small fraction of hematite is confirmed for some samples but in all cases the magnetization is dominated by minerals of the magnetite family. We further checked the reversibility of the heating and cooling curves up to 550°C, which is the highest temperature reached in our intensity experiments. Good overall stability of the magnetic mineralogy is observed during the thermal treatment (Figure 4). This is undoubtedly a favorable behavior for intensity experiments.

5.2. TRM Anisotropy

[18] The anisotropy correction factors measured for our samples at two different temperatures do not depend on the temperature at which they were determined. For ~75% of the sample collection, the difference between the two values is <2%, and in all cases <6% (Figure 5a). These variations

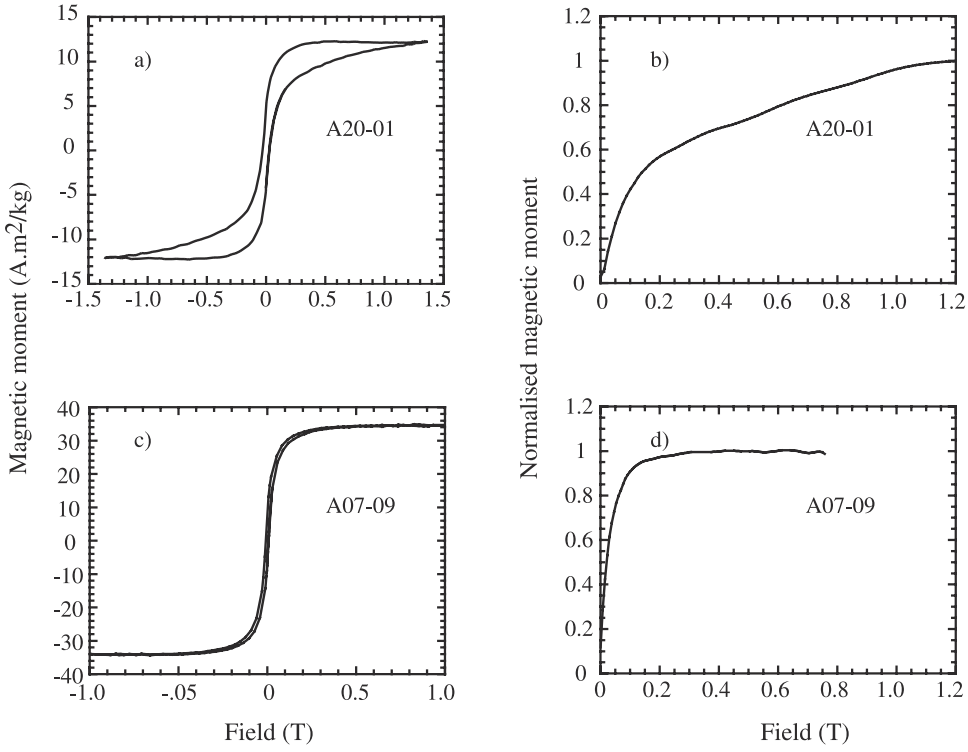

Figure 3. (a, c) Examples of hysteresis loops and (b, d) IRM experiments for ancient potsherds.

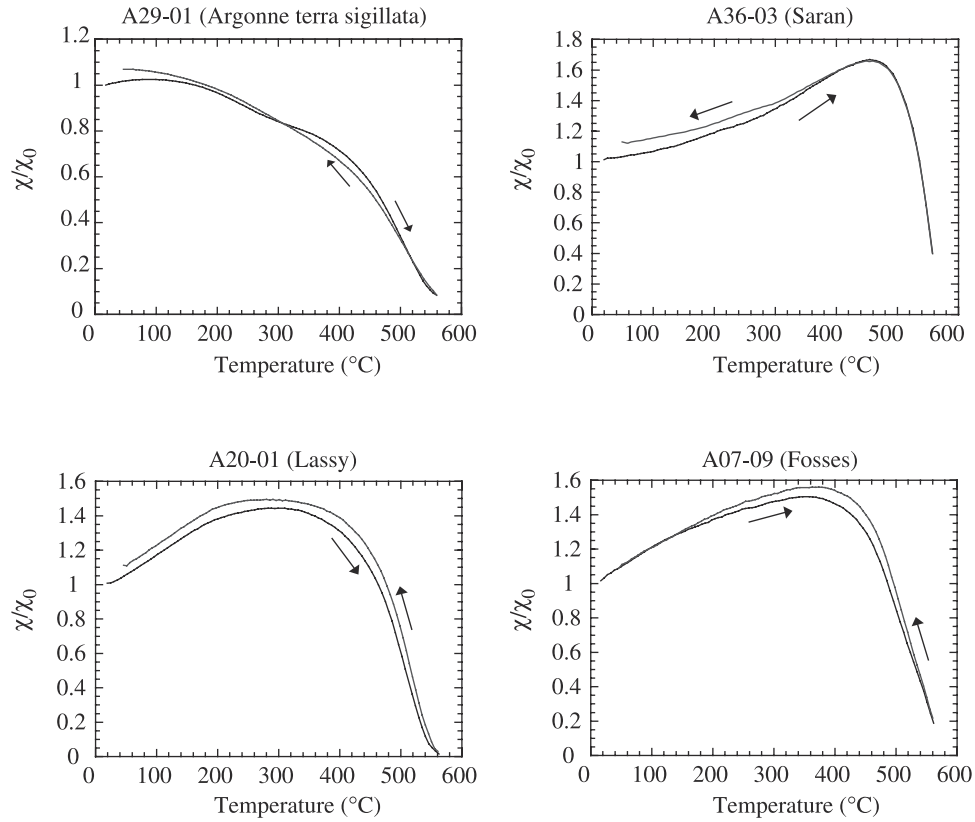

Figure 4. Normalized bulk susceptibility versus temperature curves obtained for different pottery fragments suitable for archeointensity determinations.

likely reflect small errors of sample positioning during the TRM anisotropy measurements.

[19] Our pottery samples exhibit a strong TRM anisotropy with a degree of anisotropy between 1.07 and 1.98. The highest values are obtained for a few Argonne sigillées ceramics which clearly present a clay paste with a foliated aspect. For almost all samples, the susceptibility ellipsoids have an oblate shape (i.e., K1/K2 < K2/K3 with K1, K2, and K3 being the maximum, intermediate, and minimum values, respectively), indicating that the magnetic fabric is indeed controlled by flattening. The directions of principal axes of the anisotropy tensors are generally consistent with the existence of an easy plane of magnetization identical to the shear plane of the pottery (i.e., the *x-y* plane). We mention however that this behavior is not systematic, as was previously noted by *Chauvin et al.* [2000] for bricks and tiles and by *Aitken et al.* [1981] for ceramics.

[20] The correction for the anisotropy effect was made for each sample considering the average of the two factors calculated at the two temperature steps. These mean values range from 0.97 to 1.65 and for 75% of the samples these factors are between 1.0 and 1.15 (Figure 5b). In general, the TRM anisotropy observed in two samples from the same pottery shard is very similar, with differences <5%. For only three potsherds, significant differences are observed, which likely reflect inhomogeneous stretching of the clay.

5.3. Cooling Rate Dependence

[21] As generally observed in baked clay [e.g., *Aitken et al.,* 1981; *Chauvin et al.*, 2000], the intensity of the TRM acquired after the 33 hour-long cooling is higher than the intensity of the TRM acquired after the rapid cooling for all our samples except one (see paragraph 3 and Figure 6). The overestimate (underestimate) of TRM is defined by

$$[\|\mathbf{TRM_R}\| - \|\mathbf{TRM_S}\|]/\|\mathbf{TRM_R}\| . \quad (3)$$

It varies from −2.8% to 21.4% with a mean value of ∼10% (Figure 6). This variability clearly indicates that cooling rate dependence is a critical factor which must be quantified for each ceramic fragment.

[22] To better characterize this effect, we carried out additional experiments which consisted in heating new specimens and cooling them in a field, with increasing cooling duration from 30 min to 33 hours. We refer to the 450° in 30 min cooling as the "rapid cooling rate" and to the other durations (i.e., 2, 4, 8, 16, and 33 hours) as "slow cooling rates." We also performed a rapid cooling step after each slow cooling in order to detect any alteration in magnetic mineralogy during thermal treatment. The percentage of alteration is defined by

$$[\|\mathbf{TRM_{R1}}\| - \|\mathbf{TRM_{Rn}}\|]/\|\mathbf{TRM_{R1}}\| \times 100, \quad (4)$$

where $\mathbf{TRM_{R1}}$ is the magnetization acquired after the first rapid cooling and $\mathbf{TRM_{Rn}}$ is the magnetization acquired after the nth rapid cooling following the nth slow cooling.

[23] The TRM overestimates obtained for the samples showing minor mineralogical evolution (<5%) are reported in Figure 7 as a function of the ratio of the slow versus rapid

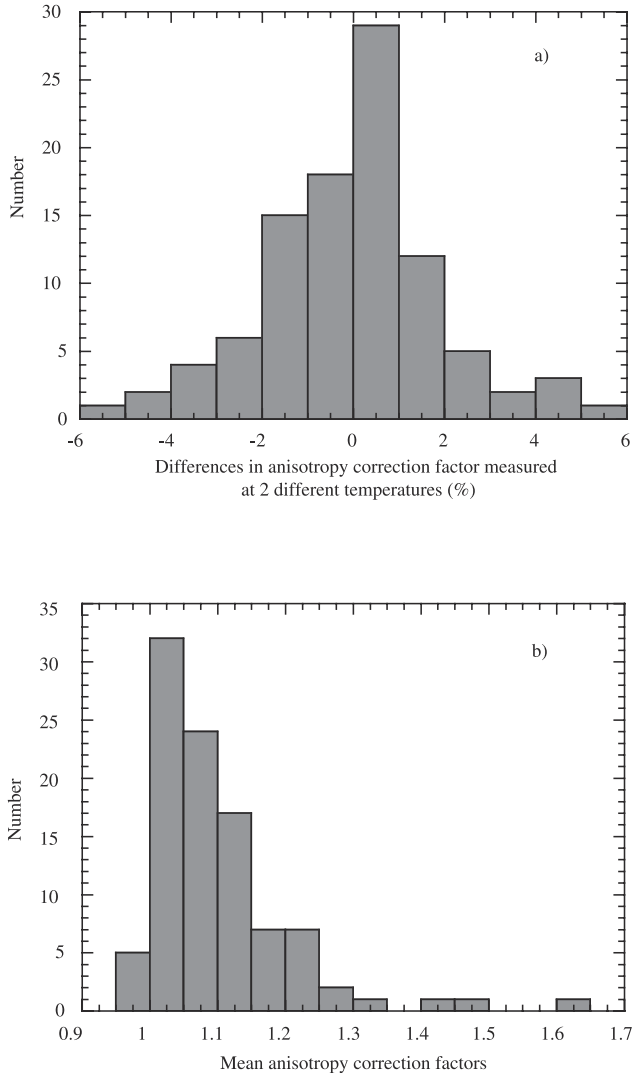

Figure 5. Determination of the TRM anisotropy correction factors. (a) Histogram of the differences in anisotropy factor measured for each sample at two different temperature steps. (b) Histogram of the mean anisotropy factors obtained for all potsherds.

cooling time (curves with symbols). We observe that for each sample the results follow a logarithmic law which underlines the thermosviscous behavior of the cooling rate effect. Such trend is expected for single domain grains [e.g., *Dodson and McClelland-Brown*, 1980; *Halgedhal et al.*, 1980] and our experiments show that it remains the same for PSD grains and for an assemblage of grains with different coercivities. We further plot the TRM over-estimate for grains with a narrow blocking temperature range near the Curie temperature derived from equation (11) of *Halgedahl et al.* [1980] (thick line, Figure 7). There is good agreement between these theoretical data and those obtained from our modern pottery fragments, although their magnetic mineralogy is much more complex. We also compared our results with some data obtained for three different potsherds by *Fox and Aitken* [1980]. For the latter study, the rapid cooling lasted 5 min and the slow cooling duration 2 hours and 16

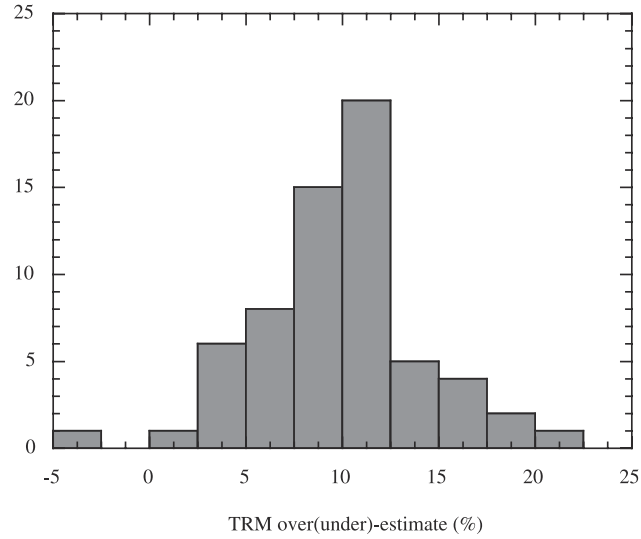

Figure 6. Histogram of the TRM over-estimates observed between a rapid cooling in 30 min and a slow cooling in 33 hours. These overestimates (expressed in percent) are defined by equation (3).

hours, which corresponds to ratios of 24 and 192, respectively. From these data, we roughly computed for each potsherd a logarithmic fit which is again compatible with our results (dashed lines, Figure 7).

[24] Altogether, our experiments demonstrate that cooling rate is a critical parameter for archeointensity determina-

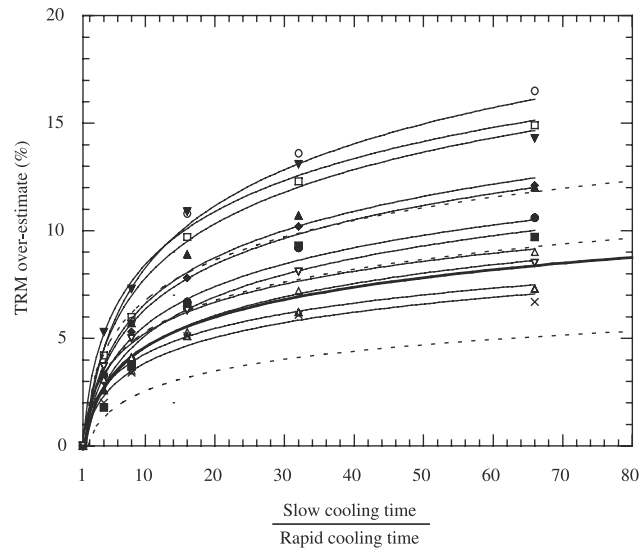

Figure 7. Evolution of the TRM over-estimates observed in several samples as a function of the ratio of increasing slow cooling duration to a fixed rapid cooling duration (see text for explanations). Each symbol represents the results obtained from one different specimen. The curves shown by solid lines are obtained by fitting the data with a logarithmic law. The curves in dashed lines are computed from the data of *Fox and Aitken* [1980] using a logarithmic fit. The thick line is deduced from theoretical computations for an assemblage of identical single domain grains [*Halgedahl et al.*, 1980].

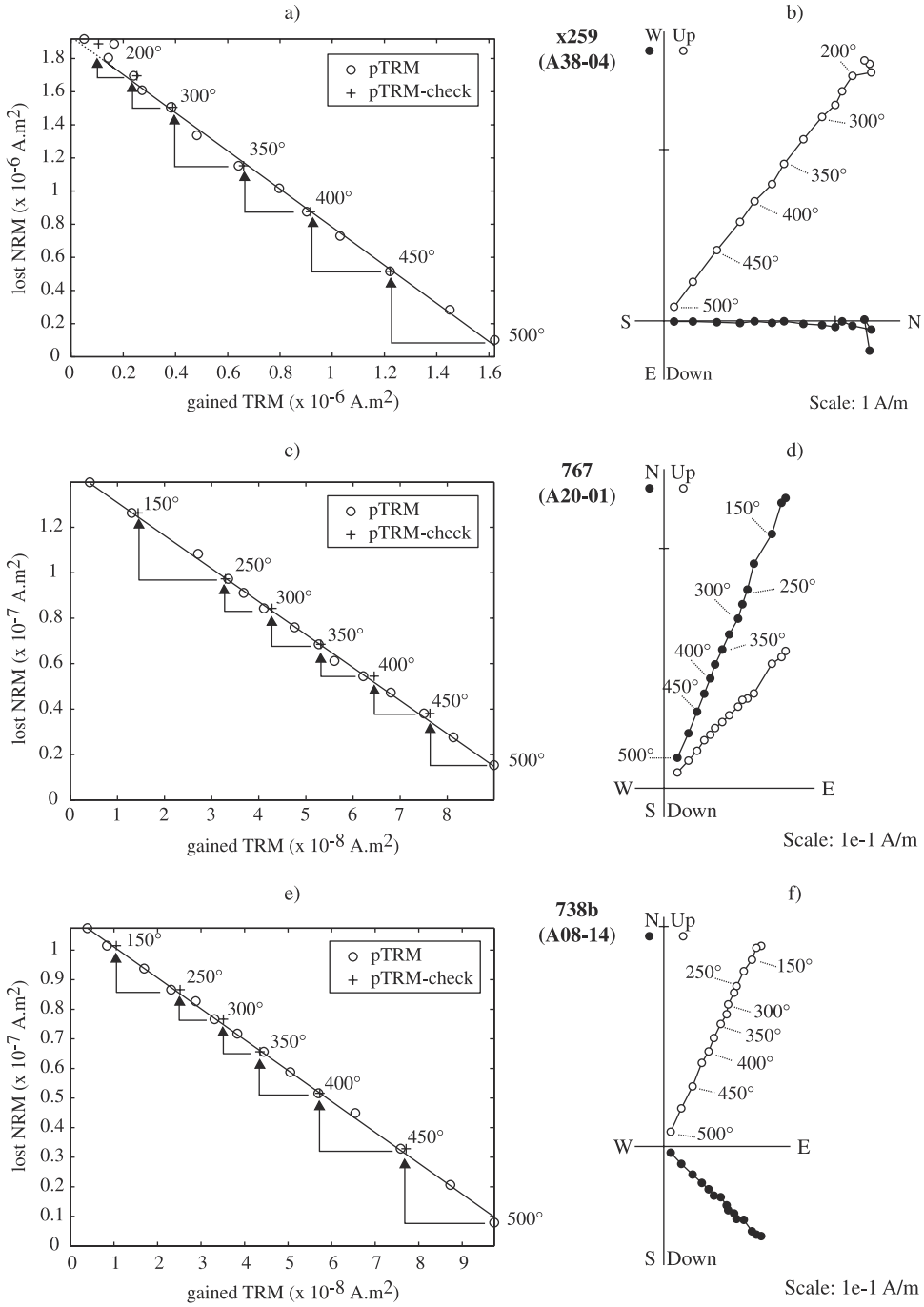

Figure 8. Examples of (a, c, e, g, i, k) NRM/TRM diagrams together with (b, d, f, h, j, l) the demagnetization curves obtained on the same samples. Same conventions as in Figure 2b are considered for the NRM/TRM diagrams. The linear segments considered for slope computations are indicated by a solid line within the temperature interval of determination and by dashed lines outside. In the demagnetization diagrams, the open (solid) symbols refer to the inclinations (declinations).

tions and that appropriate corrections are required to reproduce the original cooling conditions of the baked clays as closely as possible.

5.4. Archeointensity Measurements

[25] Six examples of NRM-TRM (Arai) diagrams are plotted together with their corresponding thermal demagnetization diagrams in Figures 8a–8l. For the majority of our accepted samples (~65%), we observe on the demagnetization diagrams a small magnetic component in the low temperature range (<200°C), which has most probably a viscous origin (Figures 8b, 8d, and 8f). This component is followed in the moderate to high temperatures by a well-defined component going toward the origin, which likely corresponds to the TRM acquired during the original firing of the ceramics. For some samples (Figures 8h and 8j), this

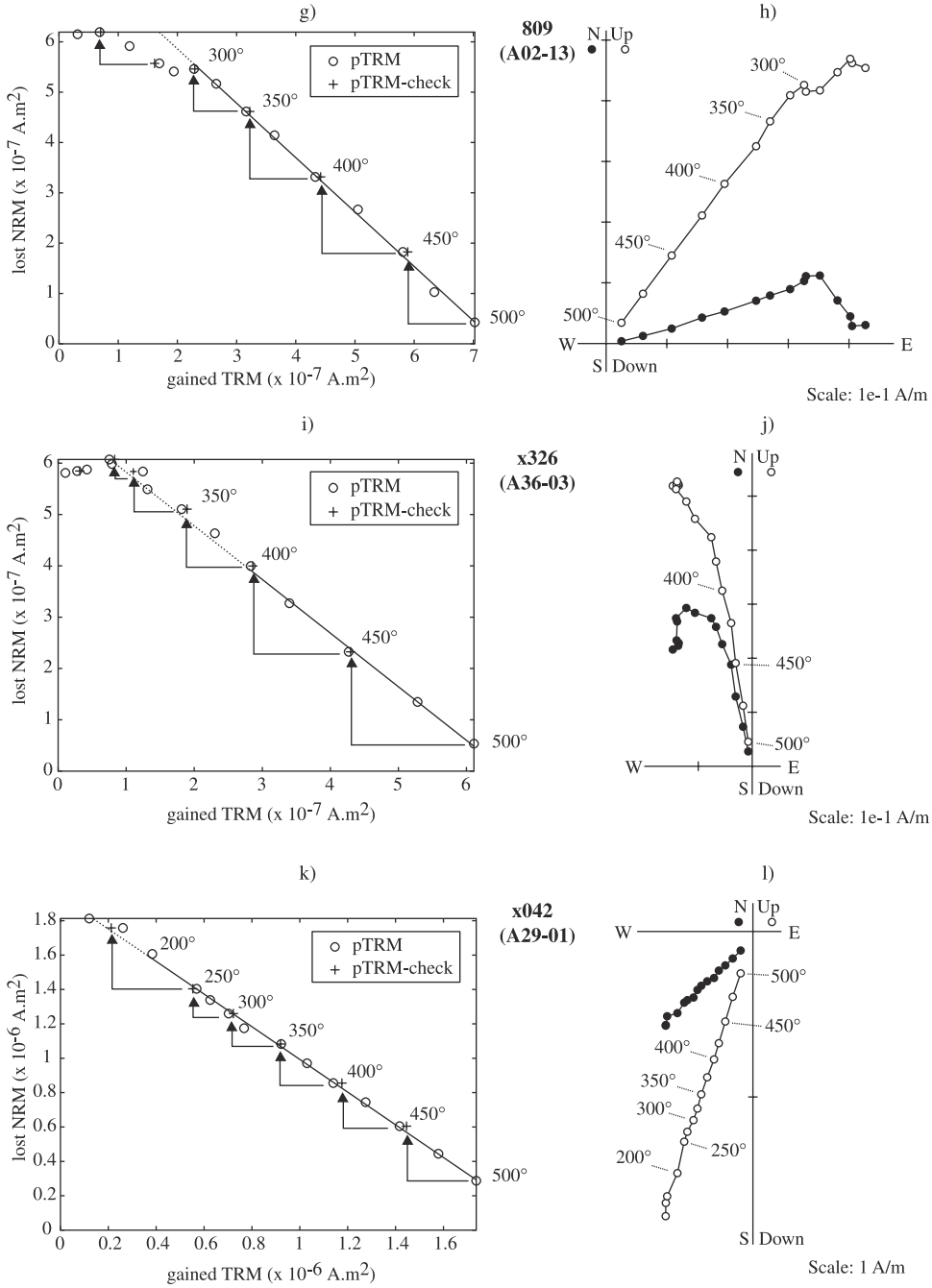

Figure 8. (continued)

latter component starts to be isolated only at higher temperatures (from 300 to 400°C), indicating that these ceramics were partially refired, thereby acquiring a small but significant secondary TRM. A few specimens exhibit a characteristic component which does not point toward the origin of the diagrams (e.g., Figure 8l). For those samples, we do not exclude the possibility that a small chemical remanent magnetization was acquired during thermal treatment. However, this (very small) spurious effect remains very limited for all accepted samples, since it does not affect significantly the linear segments in Arai diagrams, which still yield positive pTRM checks (Figure 8k). We recall here that segments were isolated in the Arai diagrams only in or within the temperature intervals selected from the demagnetization diagrams.

[26] The archeointensity results which satisfy our selection criteria are listed in Table 3. For each retained sample, we indicate the temperature interval considered for slope computation, the number of steps n performed within this interval, the NRM fraction f which provides the intensity estimate, the g gap and q quality factors as defined by *Coe et al.* [1978] and the resulting intensity with its standard error before and after correction for the anisotropy effect. We also give the mean intensity, corrected for the cooling rate computed from the average of the two intensity values obtained from the two specimens. For each studied pottery

Table 3. Archeointensity Results Obtained From Old Potsherds[a]

Potsherd	Samples	n	T_{min}-T_{max}	f	g	q	H Lab	H Non-corrected	σ_H	H Anisotropy Corrected	H Mean Value per Potsherd Corrected for the Cooling Rate Effect	$H_{mean} \pm \sigma_H$	H_{mean} in Paris	VADM, $\times 10^{22}$ A m^2	VDM, $\times 10^{22}$ A m^2
A 39: Argonne Terra Sigillata [*A.D. 325–350*]															
A39-02	X272	14	100–500	0.73	0.80	34.46	60.0	58.7	1.0	72.6	64.4 ± 1.1				
	X273	13	150–500	0.48	0.83	12.83	60.0	56.7	1.8	70.5					
A39-06	X282	11	250–500	0.53	0.89	25.62	60.0	50.0	0.9	67.0	60.5 ± 0.2	60.8 ± 3.4	60.5	9.5	10.2
	X283	11	250–500	0.57	0.89	22.29	60.0	47.4	1.1	67.4					
A39-09	X289	11	250–500	0.45	0.89	32.11	60.0	59.4	0.7	61.2	57.6 ± 0.1				
	X288	11	250–500	0.48	0.89	26.09	60.0	60.2	1.0	61.4					
A 41: Argonne terra sigillata [*400–425 A.D.*]															
A41-04	X302	14	100–500	0.85	0.90	47.23	60.0	66.3	1.1	66.9	61.8 ± 0.3				
	X303	14	100–500	0.85	0.91	46.98	60.0	66.8	1.1	67.5					
A41-06	X306	12	200–500	0.62	0.90	14.18	60.0	61.9	2.4	65.6	61.3 ± 0.3	63.9 ± 2.8	63.5	10.0	10.4
	X307	12	200–500	0.59	0.90	16.41	60.0	59.1	1.9	66.2					
A41-07	X310	13	150–500	0.78	0.89	59.01	60.0	58.8	0.7	66.1	65.4 ± 1.3				
	X311	13	150–500	0.80	0.89	60.22	60.0	63.8	0.8	68.6					
A41-08	X314	14	100–500	0.67	0.86	28.90	60.0	73.0	1.5	72.2	67.0 ± 0.6				
	X315	14	100–500	0.66	0.86	26.97	60.0	72.9	1.5	73.3					
A 29: *Argonne Terra Sigillata* [*A.D. 440–480*]															
A29-01	X042	14	100–500	0.78	0.91	50.10	60.0	57.6	0.8	71.1	64.9 ± 0.3				
	X043	14	100–500	0.76	0.91	33.37	60.0	56.8	1.2	71.5					
A29-02	X047	11	150–475	0.77	0.89	67.96	60.0	61.2	0.6	68.8	62.1 ± 0.6	62.8 ± 2.5	62.4	9.8	10.2
	X048	11	150–475	0.77	0.89	59.21	60.0	60.9	0.7	67.6					
A29-03	X050	11	250–500	0.71	0.88	47.84	60.0	44.3	0.6	73.2	64.6 ± 0.2				
	X051	11	250–500	0.72	0.88	32.82	60.0	49.5	1.0	73.5					
A29-05	X056	12	200–500	0.66	0.90	21.50	60.0	53.0	1.5	68.4	59.6 ± 0.1				
	X058	12	200–500	0.68	0.90	17.70	60.0	57.8	2.0	68.5					
A 36: Saran [*A.D. 700–750*]															
A36-01	X317	13	150–500	0.89	0.89	51.57	60.0	66.5	1.0	69.5	62.5 ± 1.7				
	X318	13	150–500	0.87	0.90	46.39	60.0	65.9	1.1	66.2					
A36-05	X328	11	250–500	0.69	0.90	38.73	60.0	63.4	1.0	69.1	64.9 ± 0.7	63.7 ± 1.1	64.3	10.1	9.6
	X329	12	200–500	0.72	0.91	55.21	60.0	62.7	0.7	70.5					
A36-06	X334	11	250–500	0.81	0.86	45.98	60.0	64.6	1.0	71.7	64.3 ± 1.0				
	X335	13	150–500	0.85	0.89	49.74	60.0	61.9	0.9	69.7					
A36-08	X338	14	100–500	0.86	0.90	88.93	60.0	68.9	0.6	69.2	63.1 ± 0.9				
	X339	11	250–500	0.80	0.88	62.45	60.0	68.8	0.8	70.9					
A 38: Saran [*A.D. 800–850*]															
A38-02	X250	13	150–500	0.88	0.91	47.41	60.0	83.5	1.4	82.2	76.1 ± 0.5				
	X252	13	150–500	0.90	0.91	48.40	60.0	83.8	1.4	81.3					
A38-04	X259	12	200–500	0.88	0.90	49.30	60.0	69.0	1.1	81.8	77.3 ± 0.4	74.7 ± 3.5	75.4	11.9	11.2
	X260	11	150–450	0.66	0.88	35.39	60.0	66.6	1.1	82.6					
A38-06	X265	13	150–500	0.82	0.90	44.09	60.0	76.7	1.3	78.2	70.7 ± 0.5				
	X267	13	150–500	0.81	0.90	43.47	60.0	74.6	1.3	77.2					
A 20: Fosses [*A.D. 920–1000*]															
A20-01	767	14	100–500	0.86	0.91	78.75	50.0	72.6	0.7	75.5	68.1 ± 0.2				
	768	14	100–500	0.86	0.91	63.36	50.0	71.6	0.9	75.9					
A20-02	773	11	250–500	0.61	0.89	24.91	50.0	64.5	1.4	69.6	61.7 ± 1.0	61.8 ± 4.5	61.7	9.7	9.7
	774	10	275–500	0.55	0.87	18.33	50.0	65.7	1.7	67.6					
A20-03	777	10	250–475	0.52	0.88	12.31	50.0	67.1	2.5	68.8	57.6 ± 1.1				
	778	11	250–500	0.63	0.89	22.31	50.0	65.7	1.6	66.7					
A20-05	784	14	100–500	0.86	0.90	40.75	50.0	67.3	1.3	69.3	59.7 ± 0.8				
	785	13	150–500	0.75	0.88	23.31	50.0	65.2	1.8	67.8					
A 02: Fosses [*A.D. 1100–1150*]															
A02-02	336	9	350–550	0.63	0.84	34.41	63.8	49.3	0.8	60.7	54.7 ± 0.1				
	337	9	350–550	0.65	0.83	27.24	63.3	51.2	1.0	60.9					
A02-10	794	14	100–500	0.78	0.91	43.33	50.0	55.1	0.9	62.3	56.1 ± 0.7	53.3 ± 2.9	53.2	8.4	8.8
	796	14	100–500	0.74	0.91	32.04	50.0	57.4	1.2	63.7					
A02-12	803	11	250–500	0.77	0.89	35.36	50.0	53.5	1.0	60.4	52.8 ± 0.3				
	804	11	250–500	0.78	0.89	39.90	50.0	53.0	0.9	61.0					
A02-13	809	9	300–500	0.66	0.87	36.32	50.0	54.3	0.9	58.6	49.5 ± 0.3				
	807	9	300–500	0.64	0.86	20.75	50.0	52.9	1.4	59.2					

Table 3. (continued)

Potsherd	Samples	n	T_{min}-T_{max}	f	g	q	H Lab	H Non-corrected	σ_H	H Anisotropy Corrected	H Mean Value per Potsherd Corrected for the Cooling Rate Effect	$H_{mean} \pm \sigma_H$	H_{mean} in Paris	VADM, $\times 10^{22}$ A m^2	VDM, $\times 10^{22}$ A m^2
							A 07: Fosses [A.D. 1200–1250]								
A07-04	636	14	100–500	0.94	0.91	91.27	50.0	54.2	0.5	58.5	56.3 ± 0.1				
	637	14	100–500	0.95	0.92	87.11	50.0	54.5	0.5	58.6					
A07-11	814	14	100–500	0.80	0.92	38.39	50.0	49.6	1.0	52.8	47.9 ± 1.0	53.3 ± 4.6	53.2	8.4	9.3
	815	14	100–500	0.76	0.92	29.90	50.0	51.8	1.2	54.7					
A07-14	709b	14	100–500	0.88	0.92	55.79	50.0	57.5	0.8	60.7	55.1 ± 0.3				
	710b	13	150–500	0.84	0.91	58.64	50.0	55.5	0.7	60.2					
A07-15	713b	12	200–500	0.68	0.88	33.43	50.0	60.7	1.1	65.9	58.2 ± 1.2				
	714b	13	150–500	0.68	0.89	59.09	50.0	56.7	0.6	63.5					
A07-17	722b	8	325–500	0.63	0.86	45.50	50.0	41.8	0.5	50.1	48.8 ± 0.3				
	721b	9	300–500	0.72	0.87	30.30	50.0	40.3	0.8	49.5					
							A 08: Fosses [A.D. 1250–1300]								
A08-02	372	14	100–550	0.92	0.92	46.47	62.7	52.8	1.0	64.4	57.1 ± 0.4				
	373	14	100–550	0.94	0.92	49.16	63.3	53.1	0.9	63.7					
A08-05	23	10	100–525	0.81	0.86	26.77	41.3	61.4	1.6	62.9	56.1 ± 0.7	54.0 ± 2.5	53.9	8.5	9.5
	24	10	100–525	0.82	0.86	25.62	41.3	60.1	1.7	61.6					
A08-13	732b	11	250–500	0.71	0.90	35.47	50.0	51.1	0.9	57.3	52.5 ± 1.0				
	733b	12	200–500	0.75	0.90	35.50	50.0	51.7	1.0	59.2					
A08-14	738b	14	100–500	0.89	0.91	90.45	50.0	52.2	0.5	55.3	51.2 ± 0.3				
	739b	14	100–500	0.90	0.92	88.12	50.0	50.5	0.5	54.8					
A08-15	741b	14	100–500	0.84	0.91	40.32	50.0	51.7	1.0	60.7	52.9 ± 0.8				
	742b	13	150–500	0.81	0.90	35.00	50.0	51.3	1.1	62.3					
							A 11: Fosses [A.D. 1300–1350]								
A11-05	367	12	250–550	0.61	0.91	34.03	63.1	52.8	0.9	52.8	48.0 ± 0.6				
	368	11	250–550	0.62	0.91	27.55	62.5	53.7	1.1	53.7					
A11-09	828	14	100–500	0.92	0.91	60.07	50.0	59.6	0.8	61.7	54.8 ± 0.2	51.8 ± 2.2	51.7	8.1	9.2
	829	13	150–500	0.86	0.90	38.54	50.0	58.8	1.2	61.4					
A11-10	832	11	250–500	0.76	0.89	71.67	50.0	50.9	0.5	60.1	54.1 ± 1.4				
	834	11	250–500	0.76	0.89	36.75	50.0	47.7	0.9	57.4					
A11-13	744b	11	250–500	0.68	0.89	47.32	50.0	56.6	0.7	58.3	51.1 ± 0.4				
	746b	9	300–500	0.64	0.87	35.77	50.0	54.7	0.9	59.1					
A11-14	748b	10	275–500	0.56	0.86	41.38	50.0	55.9	0.7	57.0	51.2 ± 0.5				
	749b	9	300–500	0.57	0.84	33.68	50.0	54.6	0.8	57.9					
							A 32: Saint Denis [A.D. 1300–1350]								
A32-01	X059	15	150–550	0.95	0.92	125.88	60.0	57.5	0.4	61.5	58.4 ± 1.3				
	X060	16	100–550	0.97	0.92	174.08	60.0	55.6	0.3	64.0					
A32-03	X066	16	100–550	0.93	0.92	70.05	60.0	61.9	0.8	65.0	59.0 ± 1.3	57.8 ± 1.5	57.8	9.1	10.3
	X069	15	150–550	0.91	0.92	87.09	60.0	58.0	0.6	67.6					
A32-04	X070	14	100–500	0.76	0.90	46.35	60.0	61.6	0.9	63.1	58.1 ± 0.8				
	X072	12	200–500	0.62	0.88	43.10	60.0	62.8	0.8	64.7					
A32-05	X076	16	100–550	0.98	0.92	51.68	60.0	57.0	1.0	62.7	55.6 ± 0.9				
	X077	14	200–550	0.95	0.92	38.19	60.0	52.2	1.2	60.9					
							A 12: Fosses [A.D. 1350–1400]								
A12-01	325	13	200–550	0.39	0.89	7.90	61.9	56.8	2.5	62.8	59.1 ± 0.1				
	324	12	200–550	0.76	0.86	31.76	62.7	58.6	1.2	63.0					
A12-03	844	13	150–500	0.83	0.90	53.86	50.0	56.7	0.8	63.2	57.7 ± 0.9	58.3 ± 0.7	58.2	9.2	10.4
	845	13	150–500	0.80	0.89	62.50	50.0	62.2	0.7	65.0					
A12-08	330	7	350–500	0.76	0.84	23.21	61.9	60.1	1.6	64.5	58.0 ± 0.9				
	331	7	350–500	0.46	0.81	11.68	64.6	60.4	1.9	62.8					
							A16: Fosses [A.D. 1500–1550]								
A16-02	412	10	325–550	0.73	0.88	25.09	64.5	47.1	1.2	54.7	57.0 ± 0.8				
	413	10	325–550	0.76	0.88	30.93	64.6	53.1	1.1	56.3					
A16-03	356	11	100–475	0.61	0.89	38.67	61.9	61.2	0.9	60.6	57.3 ± 1.0	53.0 ± 4.9	52.9	8.3	8.6
	357	11	100–475	0.64	0.89	26.11	62.6	51.5	1.1	58.7					
A16-07	414	13	200–550	0.77	0.91	42.84	64.6	43.5	0.7	49.2	48.5 ± 0.8				
	415	13	200–550	0.83	0.90	64.14	64.6	46.2	0.5	50.8					
As16-08	307	13	200–550	0.66	0.90	36.55	64.4	48.6	0.8	52.0	49.1 ± 0.2				
	306	11	300–550	0.57	0.87	27.63	64.4	48.5	0.9	52.4					

Table 3. (continued)

Potsherd	Samples	n	T_{min}-T_{max}	f	g	q	H Lab	H Non-corrected	σ_H	H Anisotropy Corrected	H Mean Value per Potsherd Corrected for the Cooling Rate Effect	$H_{mean} \pm \sigma_H$	H_{mean} in Paris	VADM, $\times 10^{22}$ A m^2	VDM, $\times 10^{22}$ A m^2
							A 18: Fosses [A.D. 1550–1600]								
A18-01	416	13	100–525	0.88	0.91	28.59	63.5	53.4	1.5	51.8	47.5 ± 0.3				
	417	12	100–500	0.82	0.89	47.70	63.1	49.3	0.8	51.3					
A18-02	853	6	350–475	0.45	0.80	11.46	50.0	53.2	1.7	55.3	44.9 ± 0.5	48.5 ± 2.4	48.4	7.6	7.7
	856	6	350–475	0.42	0.80	7.35	50.0	50.5	2.3	54.3					
A18-03	346	14	100–550	0.96	0.90	34.83	64.6	53.6	1.3	54.1	48.7 ± 0.0				
	347	14	100–550	0.96	0.90	58.10	64.6	54.1	0.8	54.1					
A18-05	X382	12	200–500	0.57	0.90	81.62	50.0	56.3	0.4	56.0	50.8 ± 1.1				
	X384	12	200–500	0.62	0.90	74.68	50.0	57.0	0.4	58.1					
A18-06	350	11	100–475	0.73	0.90	34.36	64.6	47.8	0.9	53.1	50.4 ± 0.5				
	351	14	100–550	0.96	0.92	68.79	64.6	49.1	0.6	54.0					

[a] Same column headings as Table 2. We also reported the mean intensity reduced to the latitude of Paris (48.9°N) in μT and the corresponding VADM and VDM.

group, a mean intensity and its standard deviation is computed giving the same weight to each retained pottery fragment. We indeed consider that in so far as the samples fulfill all our selection criteria, they are equivalent with respect to their ability to provide a reliable archeointensity information. Finally, we present the virtual axial dipole moments (VADM) and the virtual dipole moments (VDM) derived from our results. To determine the VDM, we computed the mean inclination within the window of age uncertainty for each pottery group using the directional data available in France for the last 21 centuries [*Bucur*, 1994; *Daly and Le Goff*, 1996].

6. Discussion

6.1. Intensity Behavior in Western Europe

[27] Our data show that the strength of the geomagnetic field rapidly varied during the High Middle Ages, with a narrow bell shape behavior in the 8th and 10th centuries (Figure 9). Peak rates of change as fast as ~7 μT per century are observed in the 8th and early 10th centuries. Although our data do not confirm the low intensity values (~25–30 μT) during the 12th century proposed by *Games and Davey* [1985] from British ceramics [see *Chauvin et al.*, 2000, Figure 13], a strong decrease by ~30% is observed between the first half of the 9th century and the 12th century (Figure 9). Such rapid changes in geomagnetic field intensity during stable polarity intervals on timescale of a few centuries were already proposed from archeomagnetic studies [e.g., *Games*, 1979; *Shaw*, 1979; *Barbetti*, 1983]. As pointed out by *Merrill et al.* [1996], this is not surprising because the magnitude of the present-day geomagnetic field changes at certain latitudes in the southern hemisphere by more than a factor 2 over 360° of longitude, which indeed gives some insight on the possible local contribution of the fast varying nondipole field on the global geomagnetic field (but see below).

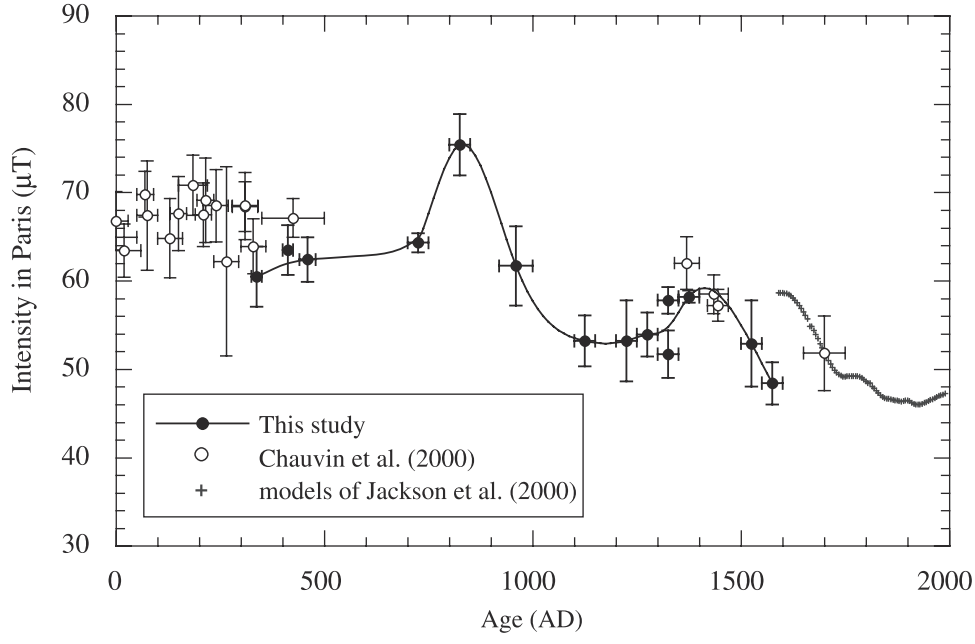

Figure 9. Evolution of the geomagnetic field intensity in France during the last 2 millennia from archeomagnetic data [*Chauvin et al.*, 2000; this study] and geomagnetic field models [*Jackson et al.*, 2000].

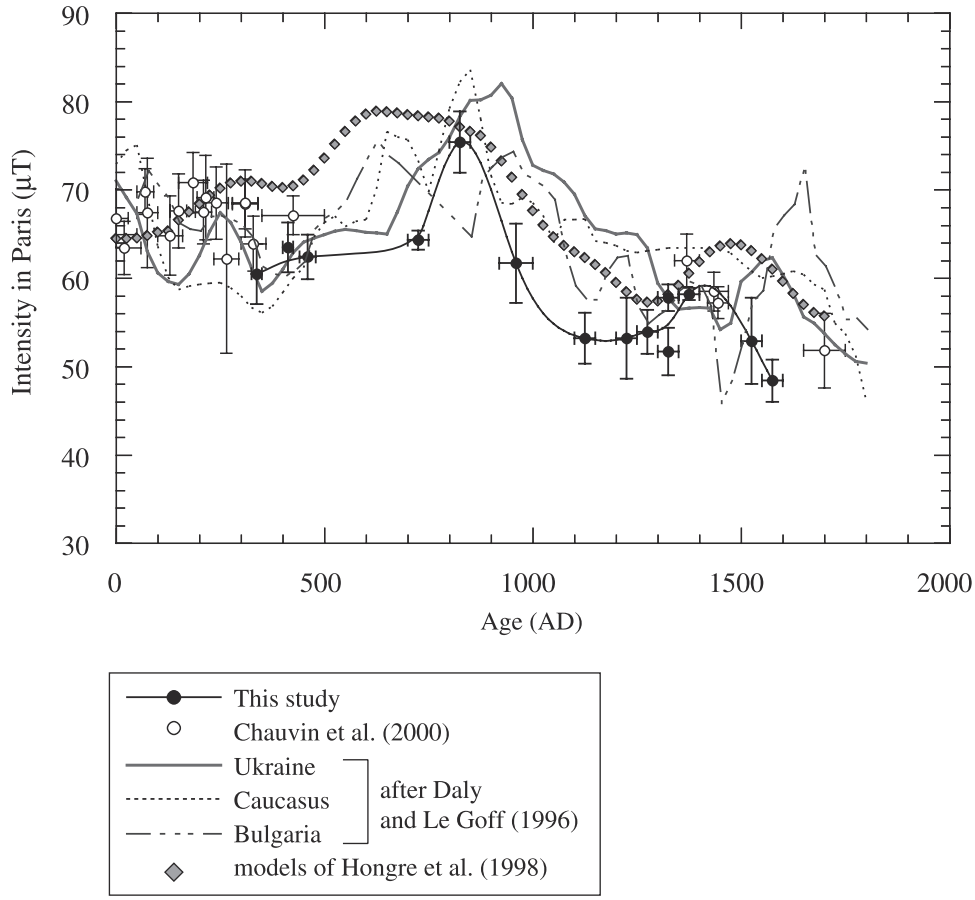

Figure 10. Comparison between the archeointensity results available in France during the last 2000 years and other data obtained in Bulgaria, Ukraine, and Caucasus smoothed over 80 year long intervals shifted every 25 years [after *Daly and Le Goff*, 1996]. For better visibility, we did not indicate the error bars of the determination of the eastern European data. The intensities derived in Paris from the *Hongre et al.* [1998] models established between 0 and A.D. 1700 are also reported.

[28] The new results also show the occurrence of a second, smaller, narrow bump in intensity during the 14th and 15th centuries (Figure 9). They are in good agreement with the few data obtained from France by *Chauvin et al.* [2000] (see also *Garcia* [1996]; open circles in Figure 9) for the 14th and 18th centuries. The latter determined from bricks and tiles share most of the selection criteria that we used in our study and they were corrected both for anisotropy and cooling rate dependence effects. However, moderate differences of $\sim$6 μT (<10% of the observed values) are observed for the 14th century between two pairs of data of the same age (Figure 9). These differences may indicate that the bump in intensity was in fact of higher amplitude but the dating accuracy of the studied materials is not sufficient to clearly resolve the rapid intensity fluctuations. A second explanation (not excluding the first one) is related to the cooling rate effect, as outlined above. In the *Chauvin et al.* [2000] study, the cooling rate dependence of TRM acquisition was quantified considering a slow cooling time of 10 hours. This duration, likely much shorter than the original one, may provoke an under-estimate of the cooling rate effect in the *Chauvin et al.* [2000] study.

[29] When our data are compared to the intensity curve derived from the historical geomagnetic field models of *Jackson et al.* [2000], we observe a large discrepancy for the 17th century, which according to the models should be characterized by a rapid decrease in intensity by $\sim$7 μT (Figure 9). Because direct intensity measurements became available only around 1830–1840, *Jackson et al.* [2000] could not constrain their model from direct inversion procedure prior to this time. They noted that the axial dipole component from 1840 to the present had decayed almost linearly at a rate of $\sim$15 nT/yr [*Barraclough*, 1974; *Bloxham et al.*, 1989] and extrapolated that rate backward, leading to the estimates shown by crosses in Figure 9. The difference above may therefore challenge the evolution of the geocentric axial dipole during this period; additional archeointensity data from the 17th to 19th centuries are necessary to solve this problem. Several other archeointensity and paleointensity values of the same age were also obtained from Great Britain and southern Italy [see in *Chauvin et al.*, 2000, Figure 13]. These results are all significantly lower than our data, but they are considered as dubious by *Chauvin et al.* [2000] since they often present a low quality index.

[30] Whereas geomagnetic intensity behavior now seems well constrained for the last 1200 years, it remains more uncertain during the Roman Empire and during the first half

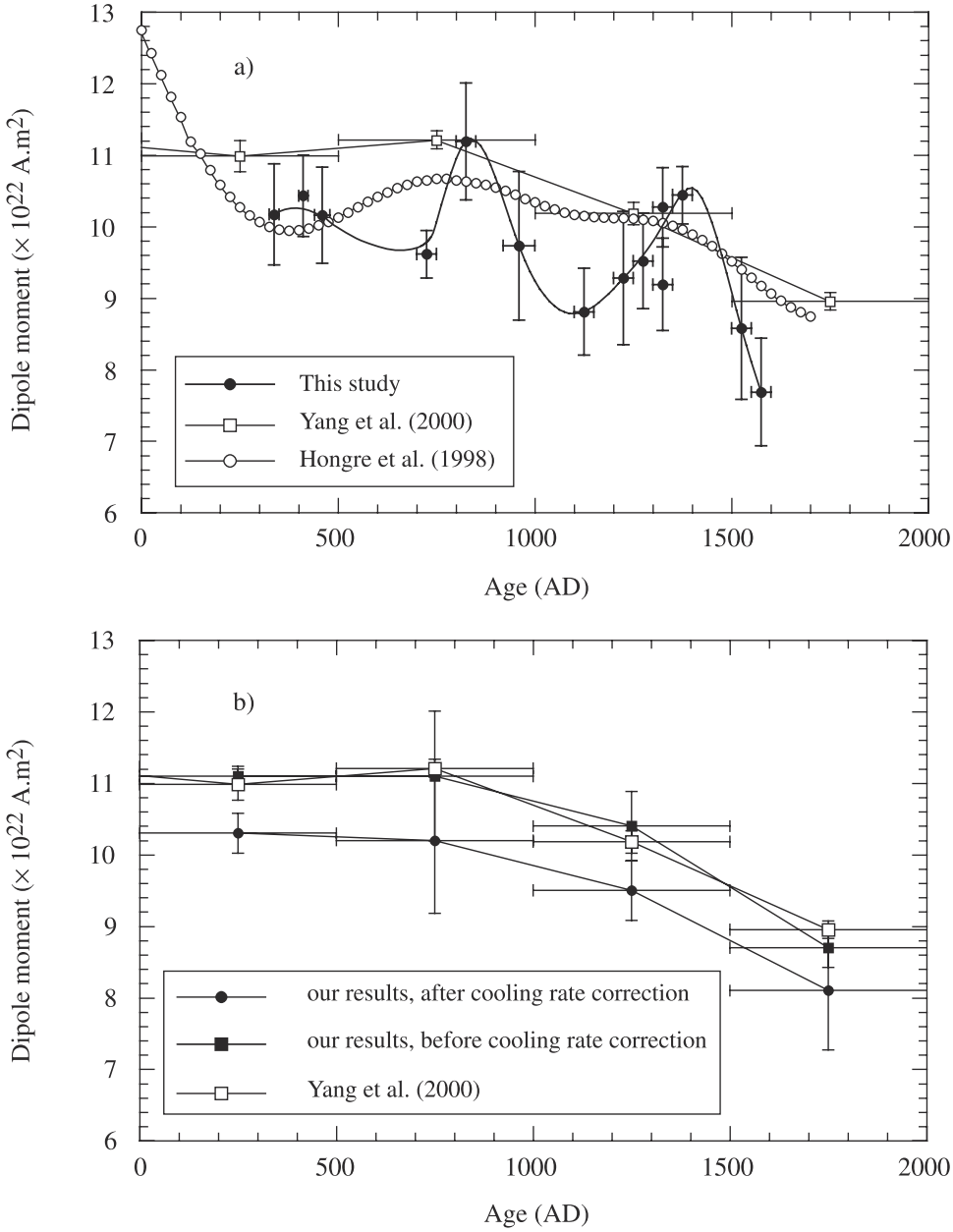

Figure 11. Comparison between our results and the evolution of the dipole field moment proposed by *Yang et al.* [2000] and *Hongre et al.* [1998]. (a) Raw data. (b) Comparison between the *Yang et al.* [2000] curve and our results averaged over time intervals of 500 years before and after correction for the cooling rate dependence of TRM acquisition.

of the High Middle Ages. The reliability of most of the many archeointensity data from the Roman period appears to be questionable [*Chauvin et al.*, 2000]. The better data are relatively scattered (Figure 9). The combined set of data [*Chauvin et al.*, 2000; this paper] may suggest a decreasing trend in intensity during the Roman period, but this possibility needs further confirmation. This period should therefore be the focus of more archeointensity studies. Another difficulty is linked to the absence of available results just after the Roman Empire, between approximately A.D. 500 and approximately A.D. 700. This corresponds to the Merovingian period for which archeological data are rare and poorly constrained in age.

[31] We briefly mention here that geomagnetic intensity fluctuations observed in western Europe during the past 2000 years offer a promising archeological dating tool. This dating method would be of particular interest for the High Middle Ages periods, for which the dating constraints based on archeological criteria often have poor accuracy.

6.2. Comparison With Other Archeointensity Results From Eastern European Platform

[32] We compared our results with the archeointensity curves from Bulgaria, Ukraine, and Caucasus [*Burlatskaya*, 1986; *Kovacheva and Kanarchev*, 1986; *Kovacheva*, 1992]. All data were treated with the same technique, i.e., a

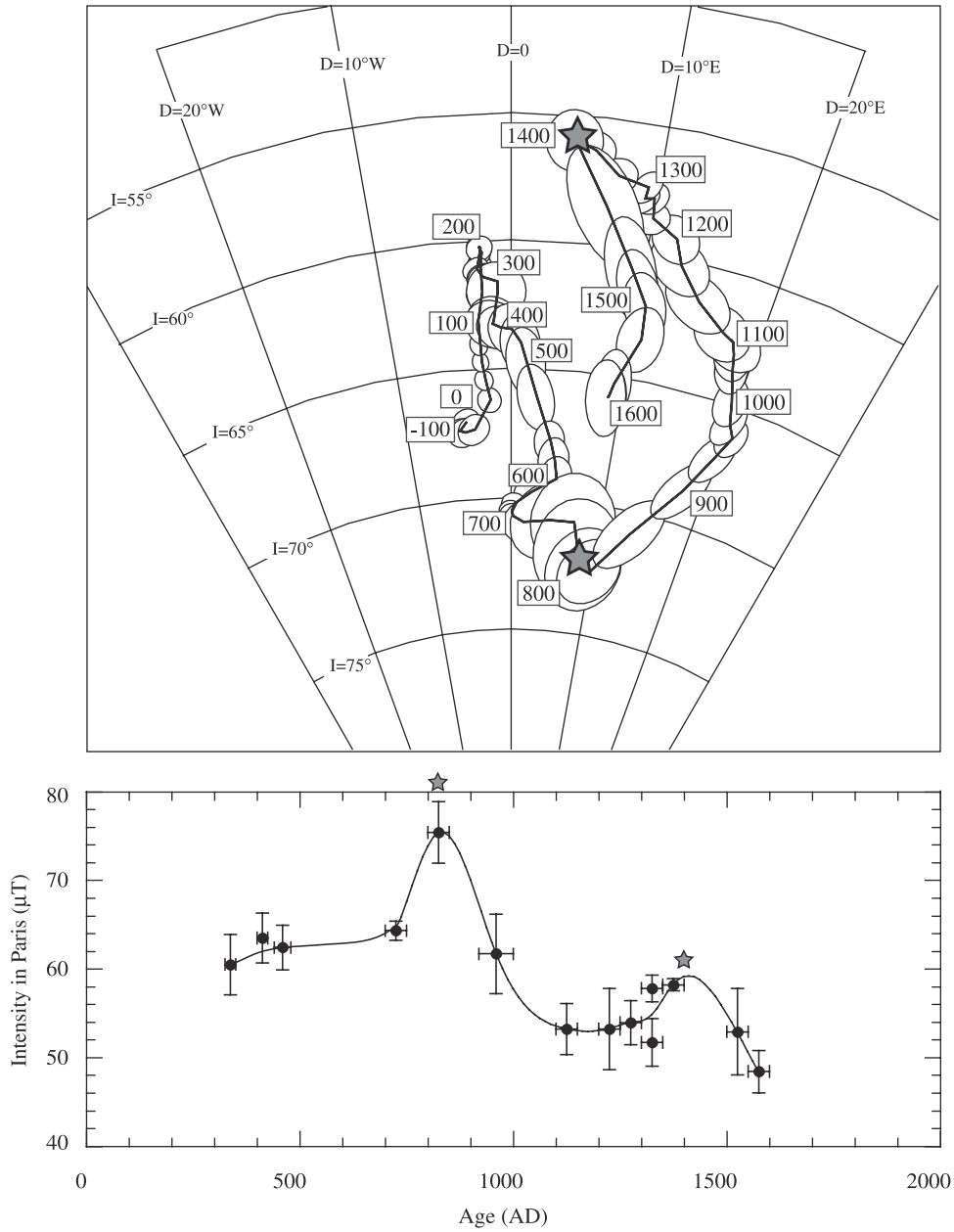

Figure 12. Directional [after *Bucur*, 1994] and intensity (this study) variations of the geomagnetic field in France obtained by archeomagnetism during the last 2000 years. Mean directions are computed using bivariate statistics over time intervals of 80 years shifted every 25 years [*Daly and Le Goff*, 1996]. The stars indicate the two bumps in intensity discussed in text.

weighted averaging over 80-year-long intervals shifted every 25 years [*Daly and Le Goff*, 1996]. Because the distances between the different regions are relatively moderate, large similarities between their respective geomagnetic intensity behaviors are expected. As a general comment, we remark that our values are generally smaller than those of others, in particular between A.D. 950 and A.D. 1350. The absence of a correction for cooling rate dependence of TRM acquisition in most earlier studies likely introduces a bias toward higher values and may explain these differences.

[33] At least for the last millennium, a shift in time of ~150 years appears between the data from France and Ukraine (Figure 10). If this shift is linked to drifting geomagnetic sources, this would indicate eastward drift of ~0.3° to ~0.1° per year between western and eastern Europe, which would have preceded the well known phase of westward drift of the nondipole field of ~0.18°/yr inferred for the "Atlantic hemisphere" from modern direct geomagnetic measurements [*Bullard et al.*, 1950; *Bloxham and Gubbins*, 1986; *Courtillot and Le Mouël*, 1988; *Merrill et al.*, 1996]. Note that archeomagnetic directions obtained from France and Ukraine also support the occurrence of dominant eastward drift during the last millennium, which is at odds with previous interpretations of archeomagnetic data [e.g., *McFadden et al.*, 1985]. In contrast, the curve

obtained from Bulgaria exhibits a complex (jagged) intensity behavior with no clear correlation with the French data (Figure 10). The curve from the Caucasus is smoother but no bump in intensity is observed during the last 500 years (Figure 10).

[34] Comparison between the different curves is difficult for the first millennium A.D. (Figure 10). The curves from Bulgaria and Caucasus may indicate the occurrence of two bumps in intensity between A.D. 500 and A.D. 1000. Our data do not have the proper time resolution to confirm this feature; a narrow intensity bump, between A.D. 500 and A.D. 750 (during the Merovingian period) could have been missed because of the lack of any data. Our data are in much better agreement with the Ukrainian curve showing a single increase in intensity during the High Middle Ages. The three east European curves may indicate the occurrence of a small bump during the Roman period, which may partly explain the apparent scatter observed in the French data.

[35] Figure 10 also shows for comparison the synthetic curve computed from *Hongre et al.* [1998] models. This curve involves some European data, but they are geographically restricted to Bulgaria, Ukraine and Caucasus. As a consequence, the comparison between our data and the expected intensity fluctuations derived in Paris from the *Hongre et al.* [1998] models exhibits to first order the same characteristics as those previously discussed (Figure 10).

6.3. Implications for Variation of the Dipole Moment and Links With Directional Secular Variation

[36] It is of interest to try to link our regional (French or western Europe) estimates of geomagnetic archeointensity with global estimates obtained from independent data sets. The important compilation of *McElhinny and Senanayake* [1982] has been recently updated by *Yang et al.* [2000]. Their results are shown in 500-year averages in Figure 11a (open squares). Because of wide geographical coverage of the data, and of the typical duration of 500 years over which most nondipole components should have been averaged out [*Hulot and Le Mouël*, 1994], these are supposed to correspond to estimates of the average axial dipole moment. They are seen to be almost constant ($\sim 11 \times 10^{22}$ Am^2) during the first millennium A.D. and to have decreased to $\sim 9 \times 10^{22}$ Am^2 over the second millennium.

[37] The model curve from *Hongre et al.* [1998] is given with much higher time resolution. It displays faster changes, with an abrupt decrease in the first four centuries, followed by several oscillations with an overall decreasing trend. If these values are averaged over 500-year windows, as *Yang et al.* [2000], the two curves will become in rather good agreement (somewhat lower by 6 μT between A.D. 500 and A.D. 1000). Our data are in good agreement with the *Hongre et al.* [1998] curve, but they show sharper fluctuations, larger maximum rates of secular variation, and overall a smaller intensity (Figure 11a).

[38] In order to smooth out part of the nondipole contribution, we performed a rough averaging of our data over time intervals of 500 years. The curve hence obtained yields a trend similar to the one proposed by *Yang et al.* [2000], although our values are significantly smaller (Figure 11b) by approximately 1×10^{22} A.m^2. However, if we had failed to correct our results for the effect of cooling rate, we would have obtained estimates essentially identical to the *Yang et al.* [2000] values (Figure 11b). Because most of the data compiled by *Yang et al.* [2000] were not corrected for cooling rate effect, we believe that their 500-year averages are significantly overestimated by $\sim$8%.

[39] It is also of interest to analyze the full geomagnetic vector, not only its intensity. If we compare the intensity variation to the directional changes determined by *Bucur* [1994] and *Daly and Le Goff* [1996], we note that the two intensity maxima observed at approximately A.D. 800–850 and approximately A.D. 1350–1400 almost coincide with two abrupt changes (cusps) in direction, possibly followed by an increase in angular velocity (Figure 12). This observation suggests, at least at the regional scale, an intriguing link between variations in direction and in intensity. Should this conjunction be other than fortuitous, we might expect a similar correlation between an intensity maximum and the approximately A.D. 200 cusp in directional secular variation. The Ukrainian data seem to point in that direction. However, this relationship is different from the simple inverse correlation between the strength of the geomagnetic field and its angular variability previously proposed by *Ohno and Hamano* [1993] and *Love* [2000]. The acquisition of new directional and archeointensity data is clearly necessary to better constrain this interesting issue.

[40] **Acknowledgments.** We are grateful to Rémy Guadagnin, who provided the potsherds from Fosses. We also thank many archeologists who helped us in collecting samples: P. Van Ossel, N. Meyer-Rodrigues, S. Jesset, N. Roy, F. Gentili, M. Cecchini, M. Hue, P. Perin, and V. Goustard. We are especially grateful to M. Le Goff, who made the new oven used in this study. We are pleased to thank L. Daly, A. Chauvin, M. Kovacheva, and G. Hulot for fruitful discussions. Special thanks to V. Courtillot, who carefully read this manuscript and made constructive comments. This study was supported by IPGP and CNRS. This is IPGP contribution 1839 and INSU 318.

References

Aitken, M., P. Alcock, G. Bussel, and C. Shaw, Archaeomagnetic determination of the past geomagnetic intensity using ancient ceramics: Allowance for anisotropy, *Archaeometry*, *23*, 53–64, 1981.

Aitken, M., A. Allsop, G. Bussell, and M. Winter, Determination of the intensity of the Earth's magnetic field during archaeological times: Reliability of the Thellier technique, *Rev. Geophys.*, *26*, 3–12, 1988.

Alexandrescu, M., V. Courtillot, and J.-L. Le Mouël, High-resolution secular variation of the geomagnetic field in western Europe over the last four centuries: Comparison and integration of historical data from Paris and London, *J. Geophys. Res.*, *102*, 20,245–20,258, 1997.

Barbetti, M., Archeaomagnetic results from Australia, in *Geomagnetism of Baked Clays and Recent Sediments*, edited by K. Creer, P. Tucholka, and C. Barton, pp. 173–175, Elsevier Sci., New York, 1983.

Barraclough, D., Spherical harmonic analysis of the geomagnetic field for eight epochs between 1600 and 1910, *Geophys. J. R. Astron. Soc.*, *43*, 497–513, 1974.

Biquand, D., Effet de la vitesse de refroidissement sur l'intensité de l'aimantation thermorémanente: Étude expérimentale, conséquence théoriques, *Can. J. Earth Sci.*, *31*, 1342–1352, 1994.

Bloxham, J., and D. Gubbins, Geomagnetic field analysis, IV, Testing the frozen-flux hypothesis, *Geophys. J. R. Astron. Soc.*, *84*, 139–152, 1986.

Bloxham, J., and A. Jackson, Time-dependent mapping of the magnetic field at the core-mantle boundary, *J. Geophys. Res.*, *97*, 19,537–19,563, 1992.

Bloxham, J., D. Gubbins, and A. Jackson, Geomagnetic secular variation, *Philos. Trans. R. Soc. London, Ser. A*, *329*, 415–502, 1989.

Bucur, I., The direction of the terrestrial magnetic field in France, during the last 21 centuries, *Phys. Earth Planet. Inter.*, *87*, 95–109, 1994.

Bullard, E., C. Freedman, H. Gellman, and J. Nixon, The westward drift of the Earth's magnetic field, *Philos. Trans. R. Soc. London, Ser. A*, *243*, 67–92, 1950.

Burlatskaya, S., *Archeomagnetic Determinations of Geomagnetic Field*

Elements, World Data, Geophys. Comm., Russ. Acad. of Sci., Moscow, 1986.
Carlut, J., and V. Courtillot, How complex is the Earth's average magnetic field ?, *Geophys. J. Int.*, *134*, 527–544, 1998.
Carlut, J., V. Courtillot, and G. Hulot, Over how much time should the geomagnetic field be averaged to obtain the mean-palaeomagnetic field?, *Terra Nova*, *11*, 239–243, 1999.
Chauvin, A., Y. Garcia, P. Lanos, and F. Laubenheimer, Paleointensity of the geomagnetic field recovered on archaeomagnetic sites from France, *Phys. Earth Planet. Inter.*, *120*, 111–136, 2000.
Coe, R., The determination of paleointensities of the Earth's magnetic field with emphasis on mechanisms which could cause non-ideal behavior in Thellier's method, *J. Geomagn. Geoelectr.*, *19*, 157–179, 1967.
Coe, R., S. Grommé, and E. Mankinen, Geomagnetic paleointensities from radiocarbon-dated lava flows on Hawaii and the question of the Pacific nondipole low, *J. Geophys. Res.*, *83*, 1740–1756, 1978.
Constable, C., C. Johnson, and S. Lund, Global geomagnetic field models for the past 3000 years: Transient or permanent flux lobes, *Philos. Trans. R. Soc. London, Ser. A*, *358*, 991–1008, 2000.
Courtillot, V., and J.-L. Le Mouël, Time variations of the Earth's magnetic field: From daily to secular, *Annu. Rev. Earth Planet. Sci.*, *16*, 389–476, 1988.
Daly, L., and M. Le Goff, An updated and homogeneous world secular variation data base, 1, Smoothing of the archaeomagnetic results, *Phys. Earth Planet. Inter.*, *93*, 159–190, 1996.
Day, R., M. Fuller, and V. Schmidt, Hysteresis properties of titanomagnetites: Grain size and composition dependence, *Phys. Earth Planet. Inter.*, *13*, 260–267, 1977.
Dodson, M., and E. McClelland-Brown, Magnetic blocking temperatures of single domain grains during slow cooling, *J. Geophys. Res.*, *85*, 2625–2637, 1980.
Dunlop, D., and Ö. Özdemir, *Rock Magnetism, Fundamental and Frontiers*, Cambridge Univ. Press, New York, 1997.
Evans, M., and L. Jiang, Magnetomineralogy of archeomagnetic materials, *J. Geomagn. Geoelectr.*, *48*, 1531–1540, 1996.
Fox, J., and M. Aitken, Cooling-rate dependence of thermoremanent magnetisation, *Nature*, *283*, 462–463, 1980.
Games, K., Short period fluctuations in the Earth's magnetic field, *Nature*, *277*, 600–601, 1979.
Games, K., and P. Davey, Archaeomagnetic determinations for Britain and south-west USA from 600 A.D. to 1700 A.D. and their implications for medieval pottery studies, *Medieval Ceram.*, *9*, 43–50, 1985.
Garcia, Y., Variation de l'intensité du champ magnétique en France durant les deux derniers millénaires, Ph.D. thesis, 353 pp., Univ. Rennes, Rennes, France, 1996.
Guadagnin, R., *Fosses-Vallée de l'Ysieux, Mille ans de Production Céramique en Ile de France,* vol. 1, *Les Données Archéologiques et Historiques*, 367 pp., Cent. De Rech. Archeol. Medievales, Caen, France, 2000.
Halgedhal, S., R. Day, and M. Fuller, The effect of the cooling rate on the intensity of weak field TRM in single domain magnetite, *J. Geophys. Res.*, *85*, 3690–3698, 1980.
Hongre, L., G. Hulot, and A. Khokhlov, An analysis of the geomagnetic field over the past 2000 years, *Phys. Earth Planet. Inter.*, *106*, 311–335, 1998.
Hulot, G., and J.-L. Le Mouël, A statistical approach to the Earth's main magnetic field, *Phys. Earth Planet. Inter.*, *82*, 167–183, 1994.
Jackson, A., A. Jonkers, and M. Walker, Four centuries of geomagnetic secular variation from historical records, *Philos. Trans. R. Soc. London, Ser. A*, *358*, 957–990, 2000.
Kovacheva, M., Updated archaeomagnetic results from Bulgaria: the last 2000 years, *Phys. Earth Planet. Inter.*, *70*, 219–223, 1992.
Kovacheva, M., and M. Kanarchev, Revised archaeointensity data from Bulgaria, *J. Geomagn. Geoelectr.*, *38*, 1297–1298, 1986.
Lanos, P., Archéomagnétisme des matériaux déplacés. Applications à la datation des matériaux de construction d'argile cuite en archéologie, 317 pp., Ph.D. thesis, Univ. Rennes, Rennes, France, 1987.
Love, J., Paleomagnetic secular variation as a function of intensity, *Philos. Trans. R. Soc. London, Ser. A*, *358*, 1191–1223, 2000.
Malin, S., and E. Bullard, The direction of the Earth's magnetic field at London, 1570–1975, *Philos. Trans. R. Soc. London, Ser. A*, *299*, 357–423, 1981.
McElhinny, M., and W. Senanayake, Variations in the geomagnetic dipole, I, The past 50000 years, *J. Geomagn. Geoelectr.*, *34*, 39–51, 1982.
McFadden, P., R. Merrill, and M. McElhinny, Non-linear processes in the geodynamo: Palaeomagnetic evidence, *Geophys. J. R. Astron. Soc.*, *83*, 111–126, 1985.
Merrill, R., M. McElhinny, and P. McFadden, *The Magnetic Field of the Earth, Paleomagnetism, the Core and the deep Mantle*, 431 pp., Academic, San Diego, Calif., 1996.
Nagata, T., Y. Arai, and K. Momose, Secular variation of the geomagnetic total force during the last 5000 years, *J. Geophys. Res.*, *68*, 5277–5281, 1963.
Néel, L., Some theoretical aspects of rock magnetism, *Adv. Phys.*, *4*, 191–243, 1955.
Ohno, M., and Y. Hamano, Global analysis of the geomagnetic field: Time variations of the dipole moment and the geomagnetic pole in the Holocene, *J. Geomagn. Geoelectr.*, *45*, 1455–1466, 1993.
Rogers, J., J. Fox, and M. Aitken, Magnetic anisotropy in ancient pottery, *Nature*, *277*, 644–646, 1979.
Shaw, J., Rapid changes in the magnitude of the archeaomagnetic field, *Geophys. J. R. Aston. Soc.*, *58*, 107–116, 1979.
Thellier, E., Sur la direction du champ magnétique terrestre en France durant les deux derniers millénaires, *Phys. Earth Planet. Inter.*, *24*, 89–132, 1981.
Thellier, E., and O. Thellier, Sur l'intensité du champ magnétique terrestre dans le passé historique et géologique, *Ann. Géophys.*, *15*, 285–376, 1959.
Van Ossel, P., La sigillée d'Argonne du Bas-Empire dans le nord de la Gaule: Distribution, imitations et concurrences (IVe-Ve s.), *Rei Cretariae Romanae Fautorum Acta*, *34*, 221–230, 1996.
Veitch, R., I. Hedley, and J.-J. Wagner, An investigation of the intensity of the geomagnetic field during Roman times using magnetically anisotropic bricks and tiles, *Arch. Sci.*, *37*, 359–373, 1984.
Yang, S., J. Shaw, and T. Rolph, Archaeointensity studies of Peruvian pottery-From 1200 BC to 1800 A. D, *J. Geomagn. Geoelectr.*, *45*, 1193–1207, 1993.
Yang, S., H. Odah, and J. Shaw, Variations in the geomagnetic dipole moment over the last 12000 years, *Geophys. J. Int.*, *140*, 158–162, 2000.

Y. Gallet and A. Genevey, Laboratoire de Paléomagnétisme, Institut de Physique du Globe de Paris, 4 Place Jussieu, F-75252 Paris Cedex 5, France. (gallet@ipgp.jussieu.fr)